Towards a Parameterizable Exoskeleton for Training of Hand Function After Stroke

Patrick Weiss*†, Lars Heyer*, Thomas F. Münte ‡, Marcus Heldmann‡, Achim Schweikard§ and Erik Maehle*
*Institute of Computer Engineering, University of Lübeck, Germany
†Graduate School for Computing in Medicine and Life Sciences, University of Lübeck, Germany
‡Department of Neurology, University of Lübeck, Germany
§ Institute for Robotics and Cognitive Systems, University of Lübeck, Germany

***Abstract*—This paper describes the mechanical design, actuation and sensing of an exoskeleton for hand function training after stroke. The frame is 3D-printed in one piece including the joints. Apart from saving assembly time, this enables parametrization of the link sizes in order to adapt it to the patient's hand and reduce joint misalignment. The joint angles are determined using Hall effect sensors. They measure the change of the magnetic field of in the joints integrated magnets achieving an average accuracy of 1.25 °. Tendons attached to the finger tips transmit forces from motors. The armature current, which is proportional to the force transmitting tendons is measured using a shunt and controlled by a custom-made current-limiter circuit. Preliminary experiments with a force/torque-sensor showed high linearity and accuracy with a root mean square error of 0.5937 N in comparison to the corresponding forces derived from the motor torque constant.**

I. Introduction

The use of the hand is ubiquitous in daily life. In case of impairment of the hand, the limited functioning can be a barrier for the sufferer. Activities of daily living may hardly be achieved, if at all. Hand impairments are among the approximately 60% most common deficits after stroke [1]. Most patients are released without full recovery. Afterwards, rehabilitation centers provide ongoing training. However, the extensive care necessary can rarely be provided due to high cost and limited manpower.

New ways of treatment are being developed to improve rehabilitation by making the therapy more effective and more efficient and by enabling home rehabilitation to allow more frequent training sessions. Robotic rehabilitation offers several advantages over traditional therapy enabling longer training sessions while decreasing the workload on therapists [2]. Sensors and actuators enhance training possibilities and allow very precise progress measurement and instant intensity adaption. Commercial hand rehabilitation devices are available like the Hand Mentor [3], [4] or the Reha-Digit [5]. The overlap of requirements for haptic and rehabilitation devices led to applications of commercial haptic systems to neurorehabilitation [6], [7].

Exoskeletons belong to the most complex rehabilitation devices due to the high number of degrees of freedom (DOF) of the hand. The complexity depends, inter alia, on the number of actuated joints, availability of bi-directional movement and accuracy of hand gesture measurement. In order to prevent excessive complexity, trade-offs have to be accepted. Worsnopp et al. developed an exoskeleton that permits independent actuation of each joint, but restricted its application to the index finger [8]. The Actuated Finger Exoskeleton AFX is used for one finger only, while focusing on high performance, real-time control with forces and speeds comparable to normal human function for motor study and rehabilitation [9]. Some devices involve every finger, but simplify the design by using one bar for the four fingers counteracting the thumb [10], [11]. The system by Fischer et al. does not allow independent finger movement either, since the cables from the finger tips are connected at the wrist for combined force transmission [12]. The CyberGrasp system was developed for haptic applications, but its functionality can also be used for rehabilitation purposes. Forces against the closing direction of the hand can be controlled independently for each finger. However, the excessive cost in a high five-digit Euro range prevents broad application in clinics and home rehabilitation.

This paper investigates the design of a hand exoskeleton for post-stroke rehabilitation, allowing virtual therapy and adaptive motor training. The system aims to be cost-efficient improving prospects in realization and commercialisation in home rehabilitation set-up. The device belongs to the m·ReS project, a **m**odular **re**habilitation **s**ystem for training of hand function.

Sensors for measuring the finger joint angles are integrated allowing interactive rehabilitation applications, the study of rehabilitation paradigms and documentation of the training progress. Actuators enable supporting or counteracting forces onto the fingers giving haptic feedback and enhancing the training possibilities.

In literature an increasing number of systems using rapid prototyping can be found. Iqbal et al. used 3D-printing for a one-fingered bi-directional underactuated prototype for daily life activity training. Based on a parametric kinematic model of the hand, Burton et al. used rapid prototyping to customize their exoskeleton to the patient's hand dimensions [13]. However, it is necessary to assemble the printed parts to a functioning system. In contrast to the aforementioned systems we print the exoskeleton as one part. This allows us to increase cost-efficiency and to introduce parametrization of the parts' dimensions to deal with the issue of misalignment.

At the present state of development, the single components are used independently. One motor is available to test functionality with one finger. The other fingers will be equipped based on the established experience. After describing the

978-1-4673-6024-1/13/$31.00 ©2013 IEEE

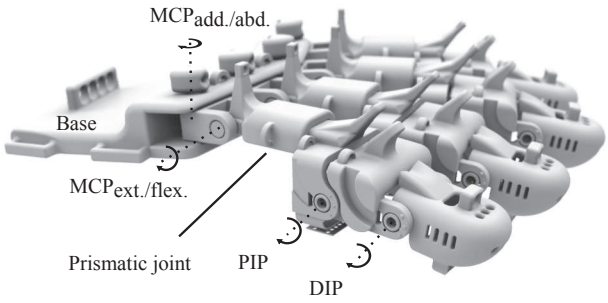

Fig. 1. Rendering of the exoskeleton with illustration of the proximal interphalangeal (PIP), distal interphalangeal (DIP) and metacarpophalangeal joints (MCP). MCP comprises two joints for adduction/abduction and extension/flexion.

design and implementation in section II, while the preliminary performance evaluation of actuator and sensors is presented and discussed in section III.

II. Design and Implementation

In this section the general design aspects are described, first with special regard to the parametrization using 3D-printing technology. The actuator with its current limiting circuit is subsequently discussed, followed by the sensors for the joint angle measurement.

A. Scope

The fingers shall be trained independently allowing adaptable force on each of the finger tips to train grasping movements. The device is intended to allow passive and active training. The present version assists in extension movements or exerts counter forces in flexion movement, respectively. Only uni-directional movement is possible within one training session. The force and angle measurements allow objective progress evaluation. Summarized into a few indicators, they document the trend of performance over several sessions.

B. 3D-Printing Opportunities and Mechanical Design

Fig. 1 shows the exoskeleton including illustrations of its joints. It includes four rotational joints per finger that correspond to the anatomical proximal interphalangeal (PIP), distal interphalangeal (DIP) and the metacarpophalangeal joint (MCP). The MCP allows flexion/extension ($MCP_{f/e}$)as well as adduction/abduction ($MCP_{ad/ab}$), why two joints with perpendicular axis are realized in the glove. The $MCP_{f/e}$ is not coaxial with the anatomical joints, which increases loading on the musculoskeletal system of the patient's hand. The prismatic joints at the links between MCP and PIP are integrated to reduce the load.

The requirements for range of motion (ROM) - 61° for MCP, 60° for PIP and 39° for DIP - are based on a functional ROM analysis by Hume et al. [14]. The palmar side of the hand is kept free so as not to inhibit finger movement, and the mechanical design allows movements almost over the full anatomical ROM. The range depends on the user, though the minimum requirements are exceeded in all cases.

The exoskeleton provides structure that transmits the forces from the motors over a tendon transmission and onto the fingers. The tendon is routed according to guides arranged in the 3D-model. The routing defines the lever arm, which determines the torques transmitted onto the finger depending on the tendon force. On one hand, longer lever arms are preferred, since smaller motors are required to provide the same amount of torque. On the other hand, applying the device in a medical environment, enormous exoskeletons can appear intimidating on patients.

We sought to strike a balance by having small lever arms spike out from the exoskeleton, while remaining enough for the tendon to touch only the guides over the whole range of movement.

Spasticity or increased muscle tone impede the usage of closed gloves. For this reason, the glove is kept open and only the finger tips are inserted in the distal link's cap. The glove's base is fixed to the hand's back using velcro.

We use 3D printing technology to adapt the exoskeleton to the patient's hand. The exoskeleton is printed as one part by leaving a gap between the rotating parts in the 3D model. The assembly effort and cost is thereby reduced. The 3D printer uses fine powder of polyamide-12 with the printed material allowing an ultimate tensile stress of $45 \pm 3N/mm^2$. With a minimum wall thickness of 2 mm at the finger links, no cracks or defects have thus far occured. The CAD/CAM process allows parametrization of the exoskeleton's part dimensions, which is discussed in more detail in the following section.

C. Parametrization

Exoskeletons have commonly presented the need to be well-aligned with the anatomy. If the mechanical joints misalign with the anatomical ones, unwanted interface forces occur that limit the voluntary range of motion and cause depression of the soft tissue. This reduces the comfort of wearing the exoskeleton from a range of uncomfortable to painful [15], [16].

Many devices use screws to adapt the link length to the user's anatomy [17]. While the adjustment is acceptable for one finger, the adaption process would be tedious to apply to the whole hand. Another approach would be to decouple joint rotations and translations, thereby achieving self-aligning of the exoskeleton axes. This, however, increases mechanical complexity and movement inertia [16].

In order to address this problem, we introduced parameters in the CAD drawing that control the dimensions of the parts. This allows customization of each exoskeleton on single users hand sizes. Conditions ensure that the parts are properly connected via the joints and that sufficient distance is maintained to prevent the 3D printer from melting parts together. The parameters are set according to the hand size of the user. At this point 38 measurements have been designed to be taken into account. The number can be reduced by introducing linear relations between the dimensions. Further parameters can be

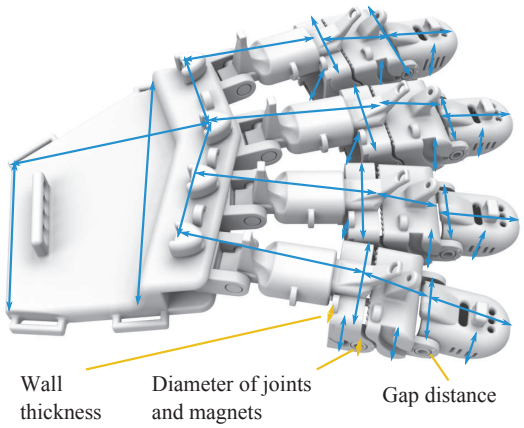

Fig. 2. Blue lines: Parameters taken from anatomy. Orange lines: Additional general parameters where applicable

adapted like the wall thickness or the separation distance in the joints. This facilitates amendments based on user feedback and parameters that depend on specifications of the 3D printer. Fig. 2 illustrates which dimensions are derived from the user's anatomy and which further parameters can be adjusted.

The parametrization process was tested on two of the authors. Dimensions for middle and ring finger were taken from the first author and index finger, pinkie and palm size were measured from the second author. The four fingers of the first prototype were adjusted according to the anatomies of both subjects. The first impressions were, that alignment was good and that the adapted finger fit significantly better, also because the anatomy differed distinctly. The printed prismatic joint sometimes jammed, which increased the load on the musculoskeletal system due to the non-coxial placed $MCP_{ext./flex.}$. The joint must be improved or a coaxial joint would be necessary. The finger width was slightly over dimensioned, which decreased the space for finger abduction/adduction. The results are subjective, but they will be used to fine-tune the parameters.

D. Actuation

The tendon force is used to adapt training to the patient's capabilities. Its measurement provides a means of assessment of the patient's motor function.

The exertion of force onto the fingers is achieved with tendons between the distal link of the exoskeleton and winders on the actuated motor shaft. Force measurements showed average force levels between 10-15N to accomplish many of our daily life activities [18]. We intend to exceed this range for the tendon forces, because the force vector is not directed in complete opposition to the finger movement direction.

We used a Faulhaber 2342 CR brushed DC motor with a nominal torque of 16 mNm and a planetary gear with a reduction ratio of 3.71:1. Due to the low ratio high backdrivability can be achieved. Previous studies showed that haptic feedback can even be implemented with higher reduction gear ratios up to 23:1 [19], [20]. With a radius r = 2.5 mm the maximum tendon force is 23.74 N according to $F = M/r$.

E. Current Limiter Electronics

Limiting the armature current allows torque control, since the two quantities are linearly related. The current limiting circuit works by switching a MOSFET that drives the motor depending on the voltage over a shunt resistor in comparison to a control voltage [21].

The circuit offers several advantages: Firstly, it needs only low reaction time to adapt rapid current changes, since the feedback is determined by linear components and no computation or control is required. The microcontroller is not involved in the feedback control, although it can influence the current by altering the control voltage with the digital-analog-converter (DAC). Special operational amplifiers with current limiting functionality exist, that are used for torque control [22]. This, however, restricts part selection, whereas the described circuit can be built with standard components.

Fig. 3 depicts the used circuit. The source and drain ports of the first metal-oxide-semiconductor field-effect transistor (MOSFET) are serially connected to the motor to switch the power through the mutual conductor. On the low-side the current is estimated via a shunt resistor with known resistance of 0.5 Ω and low tolerance of 1 %. Measuring the voltage over the shunt the current can be easily calculated according to Ohm's law. The voltage is filtered and amplified in a non-inverting configuration with the first operational amplifier (OP-AMP1). After passing the RC filter, the amplified voltage is compared with the voltage of a 10-bit digital-analog-converter (DAC) connected to a microcontroller. The amplified shunt voltage and the output from the DAC connected to a microcontroller are compared with the second operational amplifier. OP-AMP2's output is connected to the gate of the second MOSFET, which shortcuts the gate of MOSFET1. In case the amplified voltage according to the current through the motor is higher than the DAC voltage, OP-AMP2's output is maximum positive. This opens MOSFET2, which causes a voltage drop at MOSFET1's gate. The current through source and drain is minimized and, thus, also through motor and shunt. Accordingly the shunt voltage drops, while the comparison to the DAC voltage sets OP-AMP2's output to GND and therefore closes MOSFET2. This again opens MOSFET1 allowing current to run through the motor.

The safe operating current I_{max} is taken from the data sheet by calculating

$$I_{max} = \frac{M_N}{k_M} = \frac{16mNm}{56.1mNm/A} = 0.285A$$

where M_N is the nominal torque and k_M is the torque constant. The motor is supplied under the nominal voltage, so that the current lies within safe operating conditions.

F. Hall-effect angle sensor

Measurements of the finger pose are required for interactive exercises and rehabilitation progress evaluation. The measurements will be used as an extension for traditional scales to assess motor functioning like Fugl-Meyer. A encoder is mounted on the motor, so that the displacement of the tendon can be measured. However, it is not possible to determine each finger joint angle, but only a change of the tendon connected to the finger tip caused by the bending of the finger. Therefore,

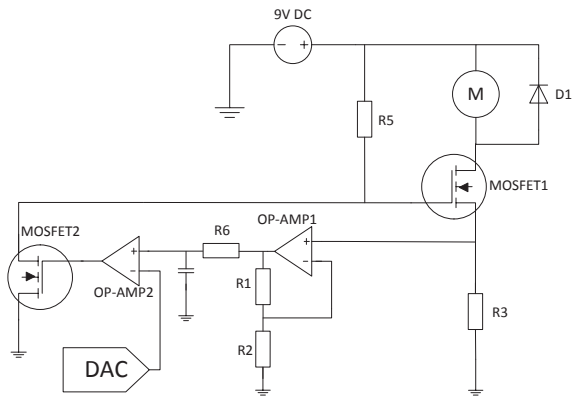

Fig. 3. Current limiting circuit

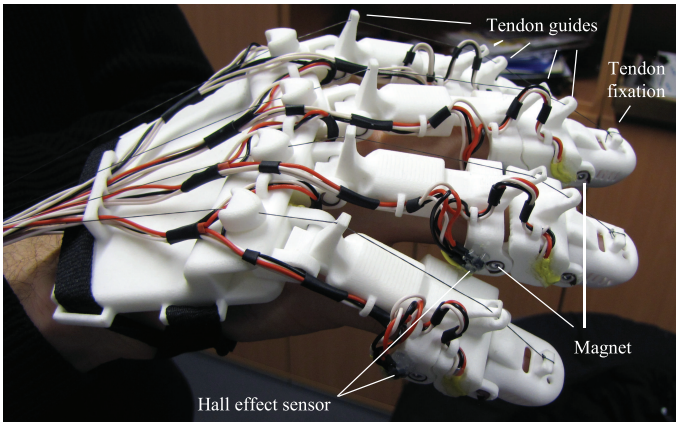

Fig. 4. Printed exoskeleton with equipped sensors donned on user

additional sensors are integrated, allowing angle measurement in each joint. Moreover, the exoskeleton's sensor do not rely on the encoder-equipped actuators.

The friction coefficient is an important parameter for any haptic device due to its effect on the sensitivity and dynamic range of the interface [23]. This in turn affects the quality of the interaction with a virtual environment. Therefore, we avoided the use of friction-inducing potentiometers.

We use Hall effect sensors for angle measurement allowing contactless measurements, so that no additional friction is caused. Based on the Hall effect, the sensor converts the surrounding magnetic field into a voltage. The sensors are placed close to magnets in the joints (see fig. 4), so that noise is minimized. By rotating the links corresponding to the joint, the magnet is rotated and its magnetic field changes. The signal of the Hall sensor relative to the angle is sinusoidal.

The exoskeleton accommodates space for the sensors and magnets. A 3D printer-dependent distance must be maintained due to manufacturing and design reasons. The initial one-time process of assembling and correctly aligning the magnet is time-consuming. The poles of the sphere-shaped magnets can be found with the help of another magnet with known pole orientation. Since the exoskeleton joints are limited in their rotation, the calibration process must be carried out before fixing the magnets in their final position. The magnets are attached so that the sensor returns unambiguous voltages over the mechanical range of motion, desirably in way that centers the ROM between U_{max} and U_{min}, so that the approximately linear voltage course lies within it.

For the angle estimation linearity is assumed. It is calibrated by measuring the voltages for 0° and 90° and by mapping the measurements to the angle by means of interpolation. The angle estimations are filtered by using a moving median over twenty samples.

III. Experiments and Performance Evaluation

The current limiting itself is first evaluated, followed by an experiment on the force production of the controlled motor. Apart from the friction losses at the contact points between tendon and routing guides, the results can be transferred to the later application, where the force on the finger tip is controlled. Afterwards, the Hall sensor angle estimation accuracy is examined. The section concludes with a discussion of the results.

A. Current limiting

1) Control voltage to current: The first experiment examines how accurate the circuit, described in subsection II-E, limits the current. Voltage from 0-5 V in 26 steps of 200 mV were applied on the minus port of OP-AMP 2 (see fig. 3) using the microcontrolled DAC. The voltage over the 0.5 Ω shunt resistor is amplified with the non-inverting amplifier with a gain of 39.17. The 10-bit ADC measures the amplified value from which the current can be calculated.

The resulting graph in fig. 6 shows a linear relationship between the control voltage and the current. The RMSE in comparison to the linear regression line is 1.7467 mA omitting the last three points. They do not follow the linear slope due to the current limitation.

2) Controlled current to force production: The following experiment examines the relation between the current measured by the ADC and the exerted force. It also allows for conclusions about the accuracy of the force estimation via current measurement by comparing the determined value with the force-torque result.

A winder was mounted onto the motor transforming the torque into a force with a lever arm of r = 2.5 mm. A tendon was winded onto the winder, which was connected to a force-torque sensor (ATI mini 45). The term "force" used in the evaluation is the Euclidean norm of the forces in x, y and z-direction measured by the force/torque sensor (see fig. 5). 100 force measurements per step were sampled and averaged.

The results can be seen in fig. 7. They are compared to motor's torque-current relation from the data sheet, which is converted into a force over the same lever arm of r = 2.5 mm. The graph shows linear behaviour with an root mean square error (RMSE) of 0.5537 N to the best-fit line and only slightly worse RMSE of 0.5937 N in comparison to the converted torque constant's slope. The points in grey are not included in the error calculation since the maximum current has been

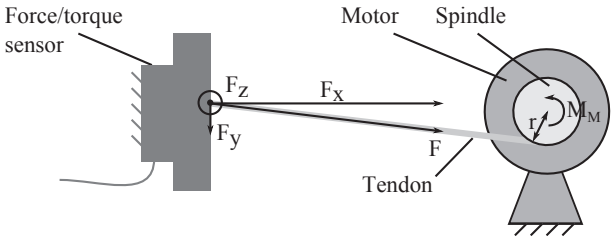

Fig. 5. Experimental setup for testing the relation between controlled current and force on tendon

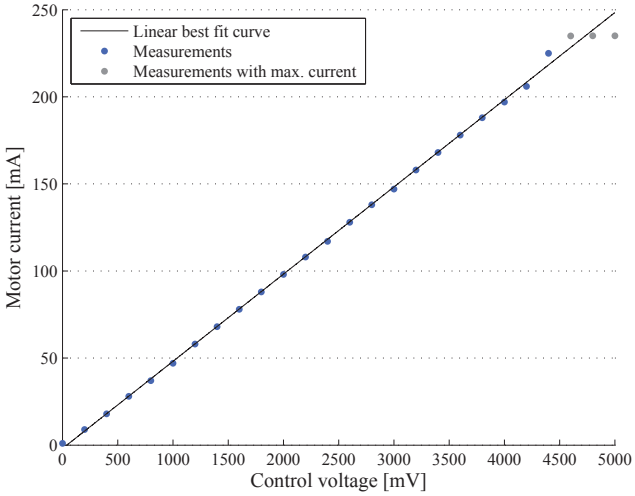

Fig. 6. Plot of DAC's control voltage against armature current measured by the microcontroller's ADC. The last three grey points are not considered for the best-fit line because the maximum current has been reached

reached and the force cannot further increase and follow the linear behavior.

Using a winder radius of 1.5 mm we achieved a maximum force of 36.1 N. However, the disturbance of the winded tendon on the lever arm is expected to be higher.

B. Angle sensor

We adjusted the exoskeleton to different orientations and measured the output of the implemented angle estimation algorithm using the Hall effect sensor. For this experiment only the index finger PIP joint was observed, because the connecting links offer space to apply the goniometer promising more accurate comparison values. Due to the manufacturing process a gap in the joint of 0.3 mm had to be regarded. The translational movement within the tolerance caused errors in the angle estimation in double-digit range. Therefore, a heat shrink tubing with a wall thickness of 0.25 mm was used to reduce the gap. Slight force was applied on the tendon in order to simulate realistic application conditions.

We used a goniometer to adjust angles from 0°to 90°in steps of 22.5°and sampled a 100 times the computed angle from the microcontroller using the Hall effect sensors and averaged it. This was repeated ten times for each angle re-adjusting the goniometer for each measurement. The results are shown in table I. The average error over all measurements is 1.25°with a standard deviation (SD) of 0.5842°.

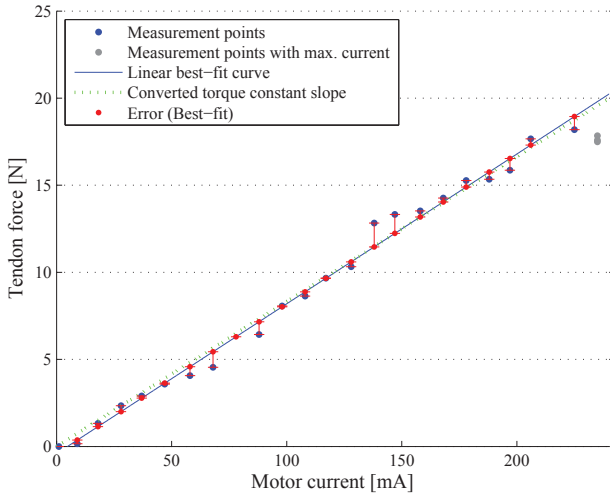

Fig. 7. Plot of controlled armature current determined with the microcontroller's ADC against tendon force measured by a force/torque sensor. The grey points are not considered for the best-fit line because the maximum current has been reached

TABLE I. ANGLE MEASUREMENT ACCURACY

Goniometer (°)	0	22.5	45	67.5	90
Microcontroller (°)	-0.28	19.64	44.12	69.26	90.47
Mean Error (°)	-0.28	-2.86	-0.88	1.76	0.47
SD (°)	0.2150	0.7970	0.4472	1.047	0.4146

Average absolute error: 1.25°
Average standard deviation: 0.5842°

C. Discussion

The current limiter circuit is able to precisely limit the current depending on the control voltage until the maximum value is reached. The plot exhibits a highly linear relation between control voltage and armature current with an RMSE of 1.7467 mA to the linear regression line.

The practical use of the circuit was shown by measuring the force exerted in dependence to the limited current. Between the armature current, controlled by the circuit and measured by the microcontroller's ADC, and the force underlies a linear relation as well. The best-fit line (RMSE=0.5537 N) and the converted torque constant's slope (RMSE = 0.5937 N) strongly coincides. The concurrence of the measurements with the theoretical value from the motor's data sheet allows to take the torque constant to estimate the force based on the current determined using the shunt resistor.

The angle measurement is used as a training and assessment device for stroke patients. Deducting friction losses, the measured force pulls at the finger tip, enabling these results to be transferred to the application. An error of 1.25°is reasonable for the intended use, especially taking the production cost and prototype state of development into the equation. From the average standard deviation of 0.5842°one can infer that it is a suitable measure for relative progress evaluation. The rehabilitation progress indicator is based on averages of several angle values, which further reduces the total error.

IV. Conclusion and Future Work

The use of 3D-printing technology enables the parametrization of an exoskeleton in order to adapt it to the user's hand and prevent misalignment of the joints. The $MCP_{ext/flex}$ is not coaxial with the anatomical joint. Although the prismatic joint accounts for this, its friction causes load on the muscoloskeletal system. A remote center of rotation joint could be an option for the future. We, however, intend on continuing to follow the manufacturing approach of a single print exoskeleton.

The performance evaluation showed that control of the force on the tendon is possible with a RMSE of 0.5937 N. Accurate control of forces onto the glove forms the basis for virtual therapy with adaptive motor training depending on the patient's needs.

The Hall effect sensor measurements offer accuracy with an average error of 1.25°. Nevertheless, reducing the joint gap required for the 3D-printing process is necessary, for example by filling the gap with a low-friction ring functioning as a plain bearing. Furthermore, in configurations where the motor encoder is available, it can be used to increase accuracy by comparing the tendon displacement with the hall sensor measurements.

So far only one motor has been used for the presented experiments and to gather experience about the interplay with the exoskeleton. The system will be extended to four motors with a separated actuation module and an extension for the thumb. Future modifications in the mechanical design will allow different configurations for further assisting flexion movement after changing the routing. This measure simplifies the design at the expense of effort for changing the training mode and not providing bi-directional movements within a session. The final goal is for a combination of the parameterizable exoskeleton, actuation and sensing presented in this paper to provide support in motor training and improvement of stroke rehabilitation.

Acknowledgment

This work was supported by the Graduate School for Computing in Medicine and Life Sciences funded by Germany's Excellence Initiative [DFG GSC 235/1].

References

[1] D. Nowak, "The impact of stroke on the performance of grasping: usefulness of kinetic and kinematic motion analysis," *Neuroscience & Biobehavioral Reviews*, vol. 32, no. 8, pp. 1439–1450, 2008.

[2] L. Pignolo, "Robotics in neuro-rehabilitation," *Journal of Rehabilitation Medicine*, vol. 41, no. 12, pp. 955–960, 2009.

[3] N. Kutner, R. Zhang, A. Butler, S. Wolf, and J. Alberts, "Quality-of-life change associated with robotic-assisted therapy to improve hand motor function in patients with subacute stroke: a randomized clinical trial," *Physical therapy*, vol. 90, no. 4, pp. 493–504, 2010.

[4] L. Rosenstein, A. Ridgel, A. Thota, B. Samame, and J. Alberts, "Effects of combined robotic therapy and repetitive-task practice on upper-extremity function in a patient with chronic stroke." *The American journal of occupational therapy.: official publication of the American Occupational Therapy Association*, vol. 62, no. 1, p. 28, 2008.

[5] H. Stefan, H. Kuhlmann, J. Wilk, C. Tomelleri, and K. Stephen, "A new electromechanical trainer for sensorimotor rehabilitation of paralysed fingers: A case series in chronic and acute stroke patients," *Journal of NeuroEngineering and Rehabilitation*, vol. 5.

[6] A. Rizzo, M. McLaughlin, Y. Jung, W. Peng, S. Yeh, and W. Zhu, "Virtual therapeutic environments with haptics: An interdisciplinary approach for developing post-stroke rehabilitation systems," in *International Conference on Computers for People with Special Needs (CPSN 05)*, 2005.

[7] B. Brewer, R. Klatzky, and Y. Matsuoka, "Visual feedback distortion in a robotic environment for hand rehabilitation," *Brain Research Bulletin*, vol. 75, no. 6, pp. 804–813, 2008.

[8] T. Worsnopp, M. Peshkin, J. Colgate, and D. Kamper, "An actuated finger exoskeleton for hand rehabilitation following stroke," in *Rehabilitation Robotics, 2007. ICORR 2007. IEEE 10th International Conference on*. IEEE, 2007, pp. 896–901.

[9] C. Jones, F. Wang, C. Osswald, X. Kang, N. Sarkar, and D. Kamper, "Control and kinematic performance analysis of an Actuated Finger Exoskeleton for hand rehabilitation following stroke," in *Biomedical Robotics and Biomechatronics (BioRob), 2010 3rd IEEE RAS and EMBS International Conference on*. IEEE, pp. 282–287.

[10] C. Takahashi, L. Der-Yeghiaian, V. Le, R. Motiwala, and S. Cramer, "Robot-based hand motor therapy after stroke," *Brain*, vol. 131, no. 2, p. 425, 2008.

[11] C. Schabowsky, S. Godfrey, R. Holley, P. Lum *et al.*, "Development and pilot testing of hexorr: hand exoskeleton rehabilitation robot," *Journal of neuroengineering and rehabilitation*, vol. 7, no. 1, p. 36, 2010.

[12] H. Fischer, K. Stubblefield, T. Kline, X. Luo, R. Kenyon, and D. Kamper, "Hand rehabilitation following stroke: a pilot study of assisted finger extension training in a virtual environment," *Topics in Stroke Rehabilitation*, vol. 14, no. 1, pp. 1–12, 2007.

[13] T. Burton, R. Vaidyanathan, S. Burgess, A. Turton, and C. Melhuish, "Development of a parametric kinematic model of the human hand and a novel robotic exoskeleton," in *Rehabilitation Robotics (ICORR), 2011 IEEE International Conference on*. IEEE, 2011, pp. 1–7.

[14] M. C. Hume, H. Gellman, H. McKellop, and R. H. Brumfield Jr, "Functional range of motion of the joints of the hand," *The Journal of hand surgery*, vol. 15, no. 2, pp. 240–243, 1990.

[15] A. Schiele, "Ergonomics of exoskeletons: Objective performance metrics," in *EuroHaptics conference, 2009 and Symposium on Haptic Interfaces for Virtual Environment and Teleoperator Systems. World Haptics 2009. Third Joint*. IEEE, 2009, pp. 103–108.

[16] A. Stienen, E. Hekman, F. Van Der Helm, and H. Van Der Kooij, "Self-aligning exoskeleton axes through decoupling of joint rotations and translations," *Robotics, IEEE Transactions on*, vol. 25, no. 3, pp. 628–633, 2009.

[17] J. Wang, J. Li, Y. Zhang, and S. Wang, "Design of an exoskeleton for index finger rehabilitation," in *Engineering in Medicine and Biology Society, 2009. EMBC 2009. Annual International Conference of the IEEE*. IEEE, 2009, pp. 5957–5960.

[18] J. Iqbal, N. Tsagarakis, and D. Caldwell, "Design of a wearable direct-driven optimized hand exoskeleton device," in *ACHI 2011, The Fourth International Conference on Advances in Computer-Human Interactions*, 2011, pp. 142–146.

[19] P. Stergiopoulos, P. Fuchs, and C. Laurgeau, "Design of a 2-finger hand exoskeleton for vr grasping simulation," *Eurohaptics, Dublin, Ireland*, pp. 80–93, 2003.

[20] J. Longnion, J. Rosen, M. Sinanan, and B. Hannaford, "Effects of geared motor characteristics on tactile perception of tissue stiffness," *Studies in health technology and informatics*, pp. 286–292, 2001.

[21] C.-K. Wei, "Torque control circuit for electrical motor," May 3 2011, US Patent 7,936,140.

[22] A. Kapoor, N. Simaan, and P. Kazanzides, "A system for speed and torque control of dc motors with application to small snake robots," in *Mechatronics and Robotics*, 2004.

[23] M. Bouzit, G. Burdea, G. Popescu, and R. Boian, "The rutgers master ii-new design force-feedback glove," *Mechatronics, IEEE/ASME Transactions on*, vol. 7, no. 2, pp. 256–263, 2002.